Development of a Velocity Model for Locating Aftershocks in the Sierra Pie de Palo Region of Western Argentina

U.S. GEOLOGICAL SURVEY BULLETIN 1795

Development of a Velocity Model for Locating Aftershocks in the Sierra Pie de Palo Region of Western Argentina

By G. A. Bollinger and C. J. Langer

Local extreme variations in sedimentary thickness required development of a velocity model to accurately compute hypocenters of the aftershock seismicity following the western Argentina (Caucete) earthquake of November 23, 1977.

U.S. GEOLOGICAL SURVEY BULLETIN 1795

DEPARTMENT OF THE INTERIOR
DONALD PAUL HODEL, Secretary

U.S. GEOLOGICAL SURVEY
Dallas L. Peck, Director

UNITED STATES GOVERNMENT PRINTING OFFICE, WASHINGTON: 1988

For sale by the
Books and Open-File Reports Section
U.S. Geological Survey
Federal Center
Box 25425
Denver, CO 80225

Library of Congress Cataloging-in-Publication Data
Bollinger, G. A.
Development of a velocity model for locating aftershocks in the Sierra Pie de Palo region of western Argentina.

(U.S. Geological Survey bulletin ; 1795)
Bibliography: p.
Supt. of Docs. no.: I 19.3:1795
1. Seismology—Argentina—Pie de Palo Mountains Region.
I. Langer, C. J. II. Title. III. Series
QE75.B9 no.1795 557.3 s 87-600225
[QE535.2A7] [551.2'2'098263]

CONTENTS

FIGURES

TABLES

Development of a Velocity Model for Locating Aftershocks in the Sierra Pie de Palo Region of Western Argentina

By G. A. Bollinger[1] and C. J. Langer

Abstract

The ten stations included in a temporary seismograph network for locating aftershocks of the November 23, 1977, western Argentina earthquake were sited where the underlying sedimentary rock columns had thicknesses ranging from 0 to 6 km (up to 1.5-sec variation in vertical one-way travel times for the P-waves). Such rapid changes in the velocity structure cause considerable difficulty in obtaining accurate hypocenter locations. Fortunately, velocity data were available in the form of 26 refraction profiles for the near surface (0–6+ km). Those profiles gave the velocities for the sedimentary column and the underlying Precambrian basement in the network area. An estimate of the regional crustal velocity structure for this geologically complex area had also been determined previously by analysis of data from a well-located nearby earthquake. Unpublished surface-wave studies extend the model to the upper mantle. This paper describes the use of the available data to refine the velocity estimates for the uppermost layers of the regional crustal velocity model and the method used to calculate P-wave travel time corrections for each station. The resulting model and station corrections were used, with good results, to locate the 185 aftershocks listed in the appendix. Average HYPO71 error measures for the aftershock hypocenters were: RMS = 0.12 sec, ERH = 0.7 km, ERZ = 1.3 km.

INTRODUCTION

The epicentral region for the magnitude 7.3 (M_s) western Argentina (Caucete) earthquake of November 23, 1977, and its aftershocks is restricted primarily to the eastern half of the Sierra Pie de Palo and to the eastern adjoining Valle Bermejo (fig. 1). That area lies within the Sierras de las Pampeanas (fig. 2) and is associated with the Sierras Pampeanas Occidentales geologic province, a region of considerable stratigraphic and structural complexity (e.g., see Allmendinger and others, 1983; INPRES, 1977; Bastias and Weidmann, 1983; Jordan and others, 1983). The resulting velocity structure varies rapidly in both the horizontal and vertical directions; consequently, the area poses serious problems to accurate earthquake hypocentral locations.

The following discussion presents a brief summary of the regional geology of the aftershock zone followed by a detailed description of a four-stage procedure used to construct a local velocity model for the aftershock locale. Development of individual station corrections to account for systematic travel time differences at each of the seismograph locations completed the velocity model study.

REGIONAL GEOLOGIC SETTING

The Sierra Pie de Palo is encircled by a system of broad valleys (Valle del Bermejo to the east and Valle de Tulum to the south and west) that form a doughnut-shaped basin (elevation of 500–700 m) filled in places with several kilometers of Quaternary age sediments. The eastern neighboring mountains, Sierra de la Huerta and Sierra de Valle Fertil as well as the central Sierra Pie de Palo, are composed of Precambrian and lower Paleozoic metamorphic and intrusive rocks that rise to more than 3,000 m above sea level. The mountain fronts are generally bounded by northerly or north-northwest-striking reverse faults that dip moderately to the east (Jordan and others, 1983; Bastias and Weidmann, 1983) but a set of crosscutting, east-northeast-trending faults and lineaments are also present (INPRES, 1977, p. 13). West of the Sierra Pie de Palo are the Paleozoic highlands that form the Andean Precordillera Centro Occidental with elevations locally in excess of 4,000 m. Reverse faulting here is extensive along both east- and west-dipping

[1]USGS and Virginia Polytechnic Inst. and State University, Blacksburg, Virginia 24061.

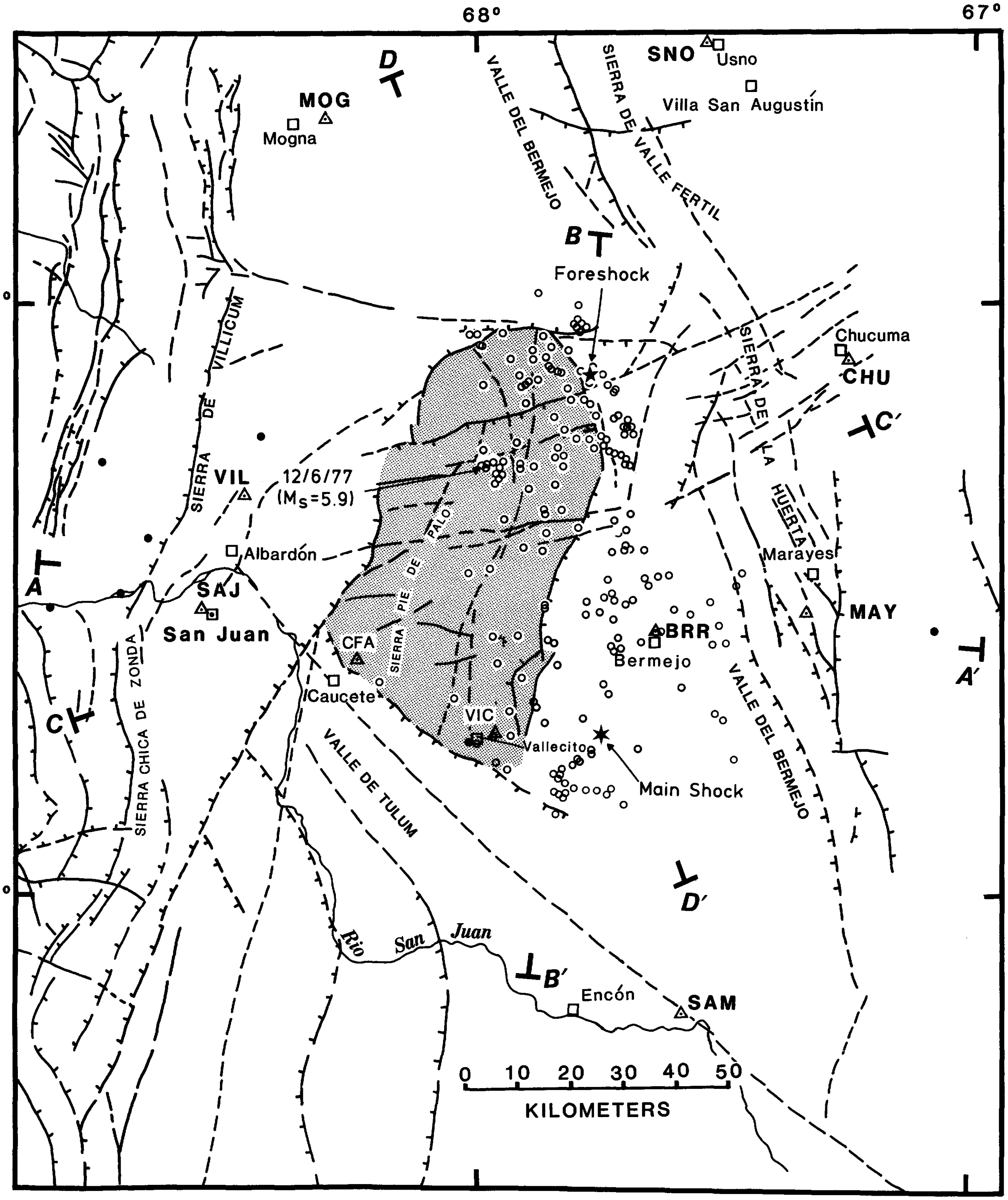

Figure 1. Aftershock epicenter (open circles) map after Langer and Bollinger (1987). Foreshock epicenter (five-pointed star) and main shock epicenter (solid six-pointed star) are from Kadinsky-Cade and others (1985); station locations shown by open triangles with center dot and three-letter station codes. Intermediate depth earthquake epicenters indicated by solid dots. Note that two of these deeper events are off the west side of the figure. Faults, shown by heavy solid (confirmed) or dashed (inferred) lines with hachures on down-dropped sides, and Precambrian outcrop on the Sierra Pie de Palo, shown by pattern symbols, were taken from INPRES (1977) geologic map. Cities and villages are indicated by open square symbols and names.

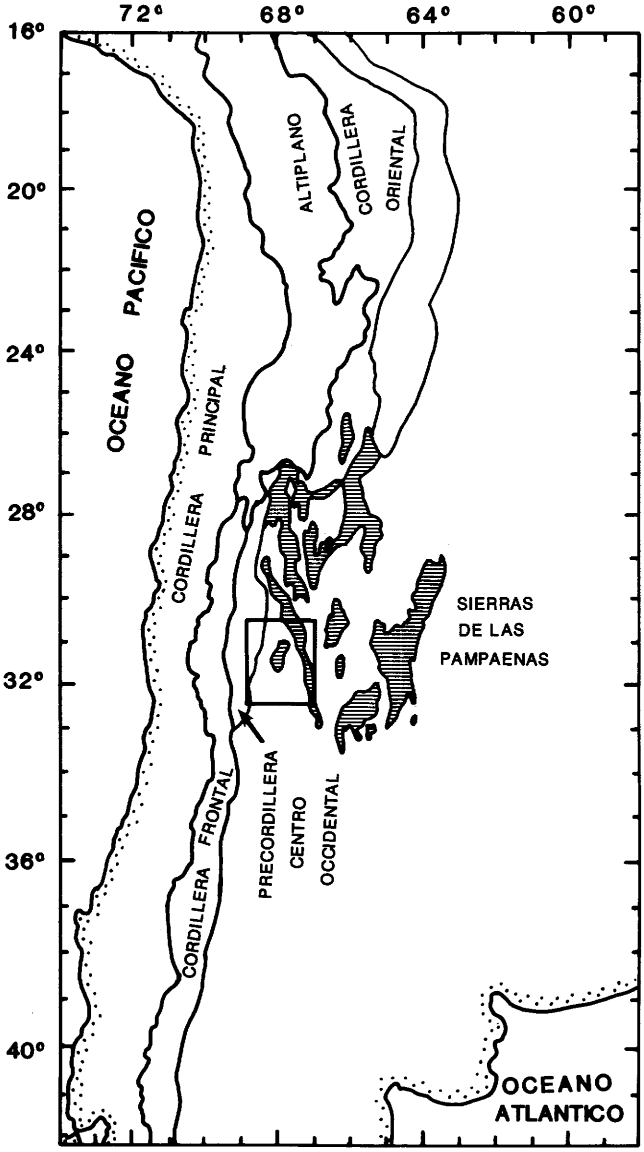

Figure 2. Location map of study area (rectangle) showing some of the geologic provinces of western Argentina. Irregularly shaped patterned figures are Sierras de las Pampaenas. The map is modified from Jordan and others (1983).

faults that predominantly strike north-south, subparallel to the Andean front. Bastias and Wiedmann (1983) have examined and described some of the major faults both east and west of Sierra Pie de Palo and have documented evidence for Holocene movement on several of the fault scarps. Baldis and Febrer (1983) have suggested that the north-northwest-striking faults just east of the Sierra Pie de Palo and the east-northeast crosscutting faults through the Sierra Pie de Palo (fig. 1) represent intersecting megafault systems that have been active from early Precambrian time to present.

DEVELOPMENT OF VELOCITY MODEL AND TRAVEL TIME CORRECTIONS

The network of eight portable and two permanent stations used to record the aftershock activity of the November 23, 1977, earthquake resulted in five stations being sited on Precambrian rocks (CFA, VIC, MAY, CHU, and SNO) and five stations on the basinal alluvium (MOG, BRR, SAM, VIL, and SAJ; e.g., see fig. 3). Given these very different station bedrock types, fortunately an approximate regional P-wave crustal-velocity model (Volponi, 1968) and results from 26 refraction profiles in the epicentral area were made available by Yacimientos Petroliferos Fiscales (YPF), the Argentine National Oil Company (see fig. 3). All but one of the YPF profiles were reversed and provided data to compute the sedimentary column and uppermost Precambrian (basement) velocities. Additionally, sonic log data from two wells that had been drilled in the northern part of the study area near 30° S., 68° W. (D. R. Toland, Cities Service Company, Houston, Tex., personal commun., 1978; fig. 3) agreed, generally, with the refraction velocity data in their vicinity. However, the wells were not drilled deep enough to extend our knowledge of the Precambrian velocities and, thus, only helped to confirm the velocity information within the section. Also, depth to the top of the mantle (Mohorovicić discontinuity), and the upper mantle velocity were estimated by J. C. Castano (staff seismologist, INPRES, San Juan, Argentina, personal commun., 1977) based on unpublished surface-wave studies.

To correct for the complexities in lithology and the other local geologic factors that affect seismic velocities, we state the following objectives and the analytic procedures to achieve these objectives:

- Develop an "average" layered velocity model (AVM) that is representative of the upper 10 km of crust in the Sierra Pie de Palo area.
- Estimate station corrections to account for systematic travel time differences at each station that result from the model.
- Estimate "station-delay" corrections that account for systematic travel time differences at each station that result from unknown sources.
- Combine the AVM station corrections with the "station-delay" corrections to estimate the "final" station corrections.

A brief summary of what the available data include is: 25 reversed and 1 non-reversed refraction profiles, well log data from 2 wells, a regional velocity model (Volponi, 1968), depth to the upper mantle and upper mantle velocity estimates from Castano, and aftershock data recorded at 10 stations. Our task is to apply these data

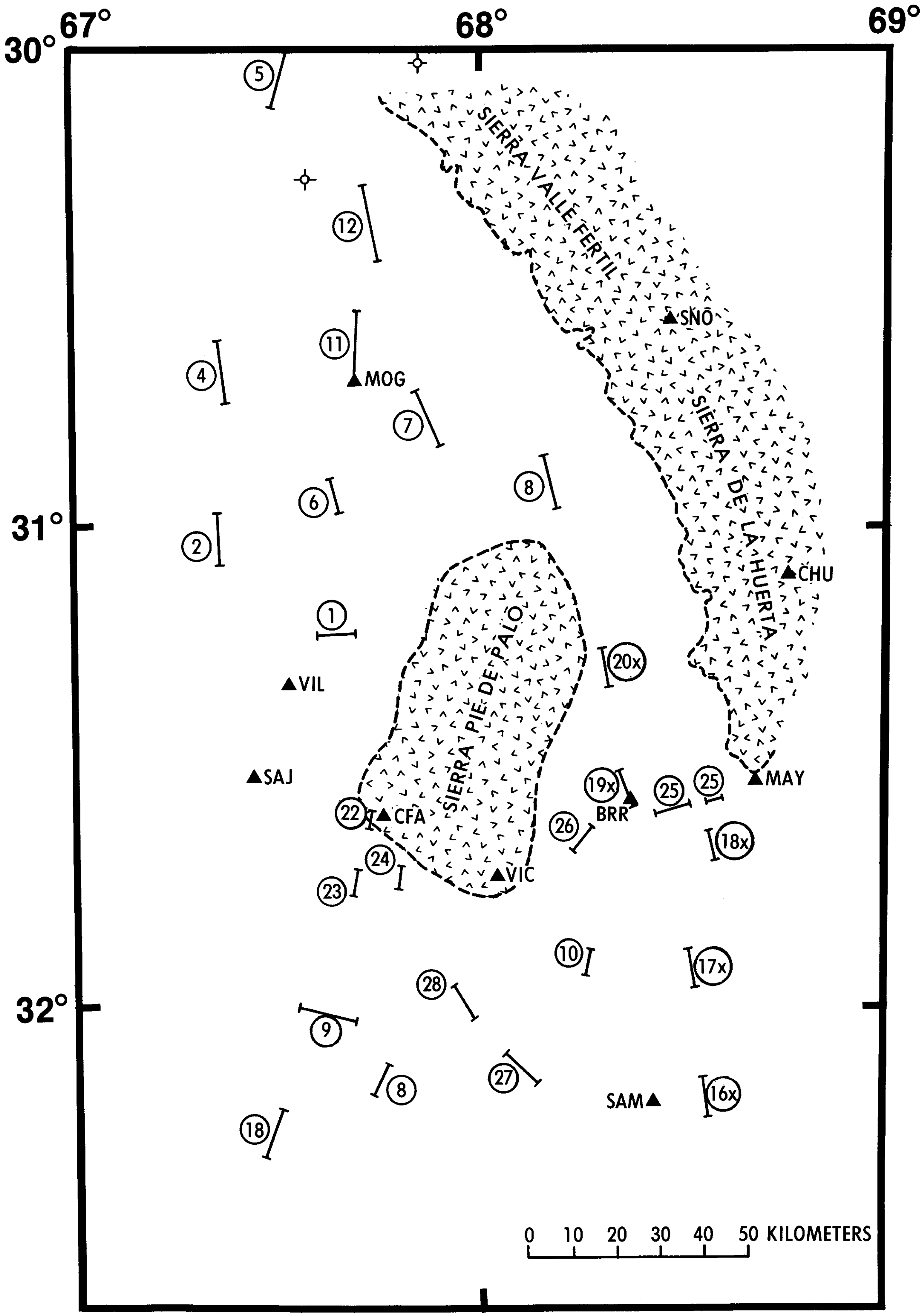
67°
68°
69°
30°
31°
32°
SIERRA VALLE FERTIL
SIERRA DE LA HUERTA
SIERRA PIE DE PALO
SNO
MOG
CHU
VIL
SAJ
CFA
VIC
BRR
MAY
SAM
1
2
4
5
6
7
8
9
10
11
12
16x
17x
18x
18
19x
20x
22
23
24
25
26
27
28
0 10 20 30 40 50 KILOMETERS

in a rational and also rigorous method to achieve the above-stated goals. A step-by-step description of how the "average velocity model" was developed and how the station corrections were determined is given below.

(1) *Average velocity model (AVM), Upper 10 km*

(a) Location, length, and direction of profiles were plotted (fig. 3).

(b) Thickness and average sedimentary-column velocities were determined for all profiles, plotted at the profile center, and contoured (figs. 4 and 5).

(c) Precambrian basement velocities were determined, found to be variable, plotted, and contoured (fig. 6).

(d) The study area was gridded at 1/4-degree intervals and, for each of the resulting 45 grid points, the sedimentary velocity (V_{sed}), sedimentary thickness (Z_{sed}), and Precambrian basement velocity (V_{pe}), were estimated by interpolation between respective contours and then plotted (fig. 7).

(e) Mean values were obtained directly for each of the parameters in figure 7 and used as representative numbers in the AVM. The generalized P-wave velocity model for the upper 10 km is then:

P-wave Velocity (km/sec)	Thickness (km)	Depth to top of layer (km)
2.87	2.4	0
5.88	7.6	2.4

Available measurements of middle and lower crustal velocities from Volponi (1968) add to our model and are as follows:

P-wave Velocity (km/sec)	Thickness (km)	Depth to top of layer (km)
6.2	22.0	10.0
7.3	?	?

The combination of our AVM with Volponi's investigation (1968) and information from J. C. Castano leads to our final P-wave velocity model given in table 1.

The model specifies only average velocities and thicknesses for the two layers above 10 km. However, looking at figures 4–8, considerable variability exists in sedimentary thickness, sedimentary velocity, and Precambrian velocity throughout the network area. Given the velocity and thickness for the AVM layers and, then, using figures 4, 5, and 6, to determine the "actual" P-wave travel time parameters for the upper two layers, we can estimate the AVM station corrections.

(2) *AVM Station Corrections, T_c*

(a) Determine vertical, one-way travel time through the upper 10 km which we call the "AVM travel time," T_m, according to values specified by the AVM.
$T_m=(2.4 \text{ km}/2.87 \text{ km/sec})+(7.6 \text{ km}/5.88 \text{ km/sec}) =0.84 \text{ sec}+1.29 \text{ sec}=2.13 \text{ sec}$

(b) Use the "AVM travel time" ($T_m=2.13$ sec) to contrast with the "actual station travel times," T_a, at each of the network stations.

(c) Calculate difference between AVM and "actual" travel times for AVM station corrections:

$$T_c = T_m - T_a.$$

Sample AVM station correction calculations are given below for a basin location (MOG) and rock location (MAY). Because of adjustments in scale and projection that were necessary to composite the several large work maps used for preparation of the illustrations, corrections derived directly from the figures presented herein may not agree exactly with those described in the following text.

T_c for MOG (Sedimentary Site)

a. From figure 8, the sedimentary travel time, $T_{sed}=1.8$ sec

b. From figure 3, the sedimentary thickness (including station elevation), $Z_{sed}=6.2$ km

c. From figure 6, the Precambrian velocity, $V_{pe}=6.0$ km/sec

d. Thickness of Precambrian above 10 km, $Z_{pe}=10.0–Z_{sed}=10.0 \text{ km}–6.2=3.8$ km

Figure 3. (facing page) Location of refraction profiles obtained from Yacimientos Petroliferos Fiscales (YPF) (Burna, Abel E., Ing., Chief, Special Studies Agency of Interpretation and Investigation, YPF, Buenos Aires, Argentina, written commun., 1978); profiles are indicated by short lines with end bars; profile numbers given inside open circle symbols are those assigned by YPF. Seismograph station locations shown by solid triangles and 3-letter station codes. Location of two wells indicated by dry-hole symbols (open circles with four tic marks). Precambrian outcrop areas shown by pattern symbol. Open area, except to the far west, represents basinal sediments.

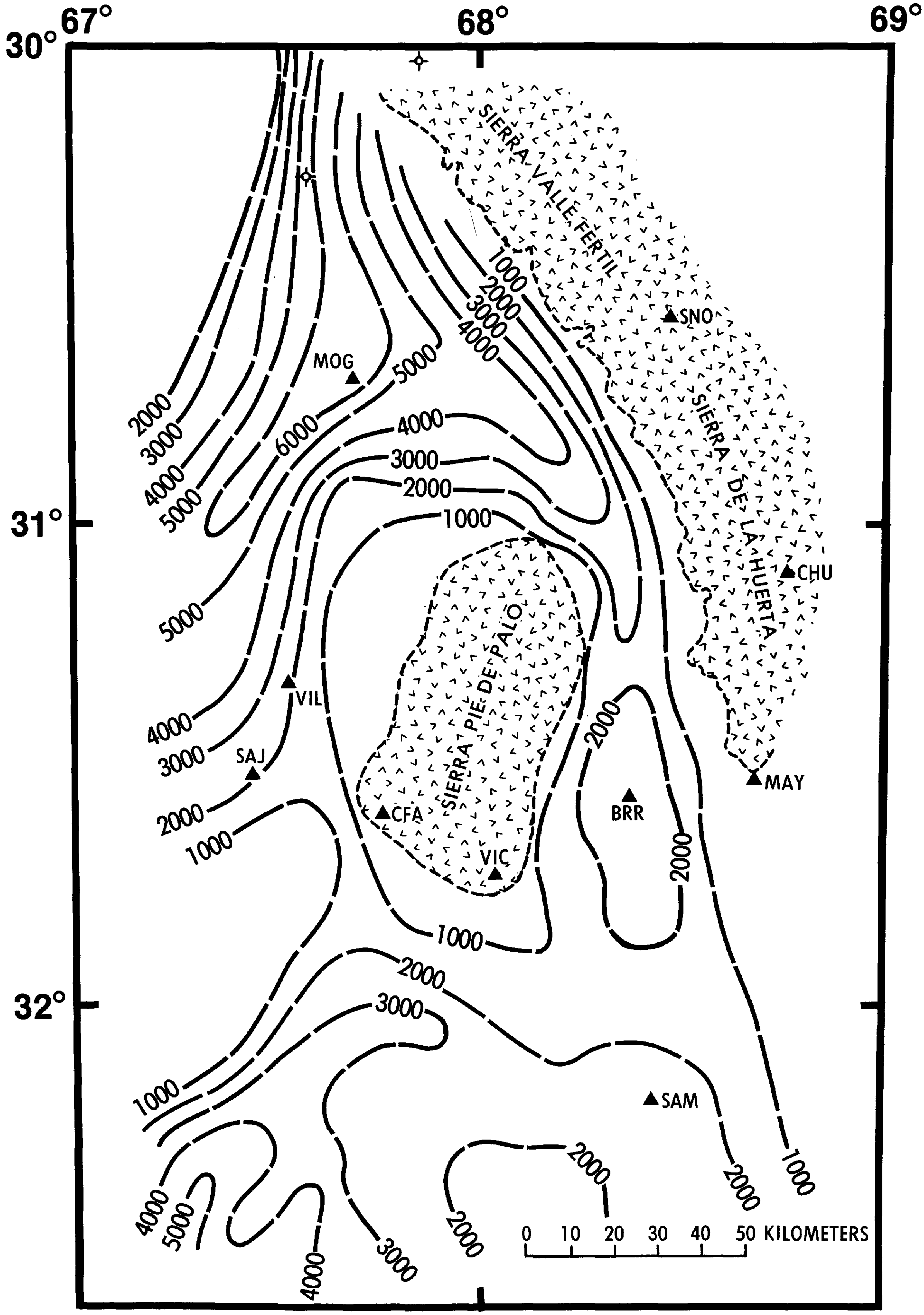

Figure 4. Thicknesses of sedimentary rocks, as calculated from the refraction profile data (fig. 3), contoured in meters. Other symbols the same as in figure 3.

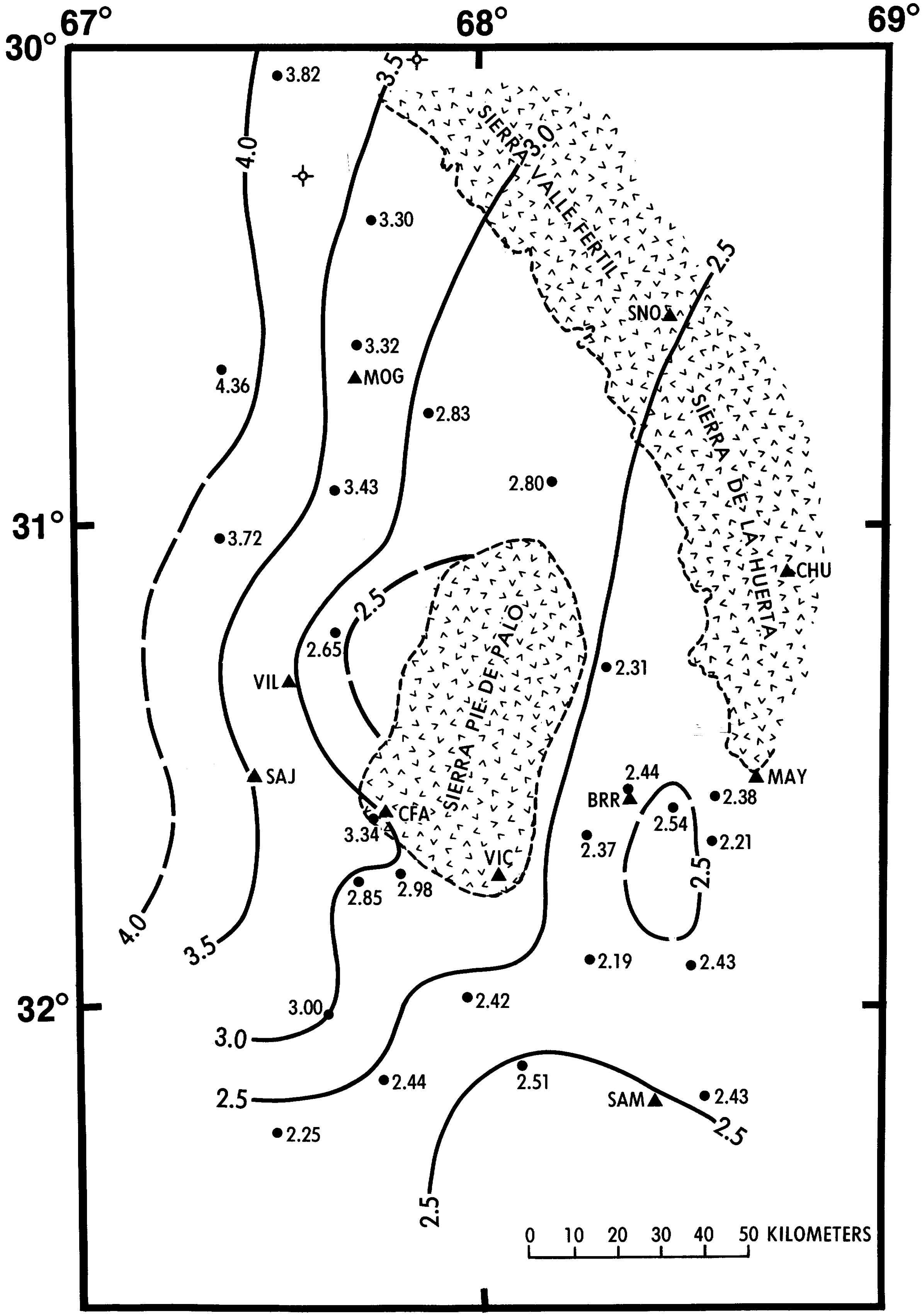

Figure 5. Average sedimentary rock velocities, as calculated from the refraction profile data (fig. 3), contoured in km/sec. Other symbols the same as in figure 3.

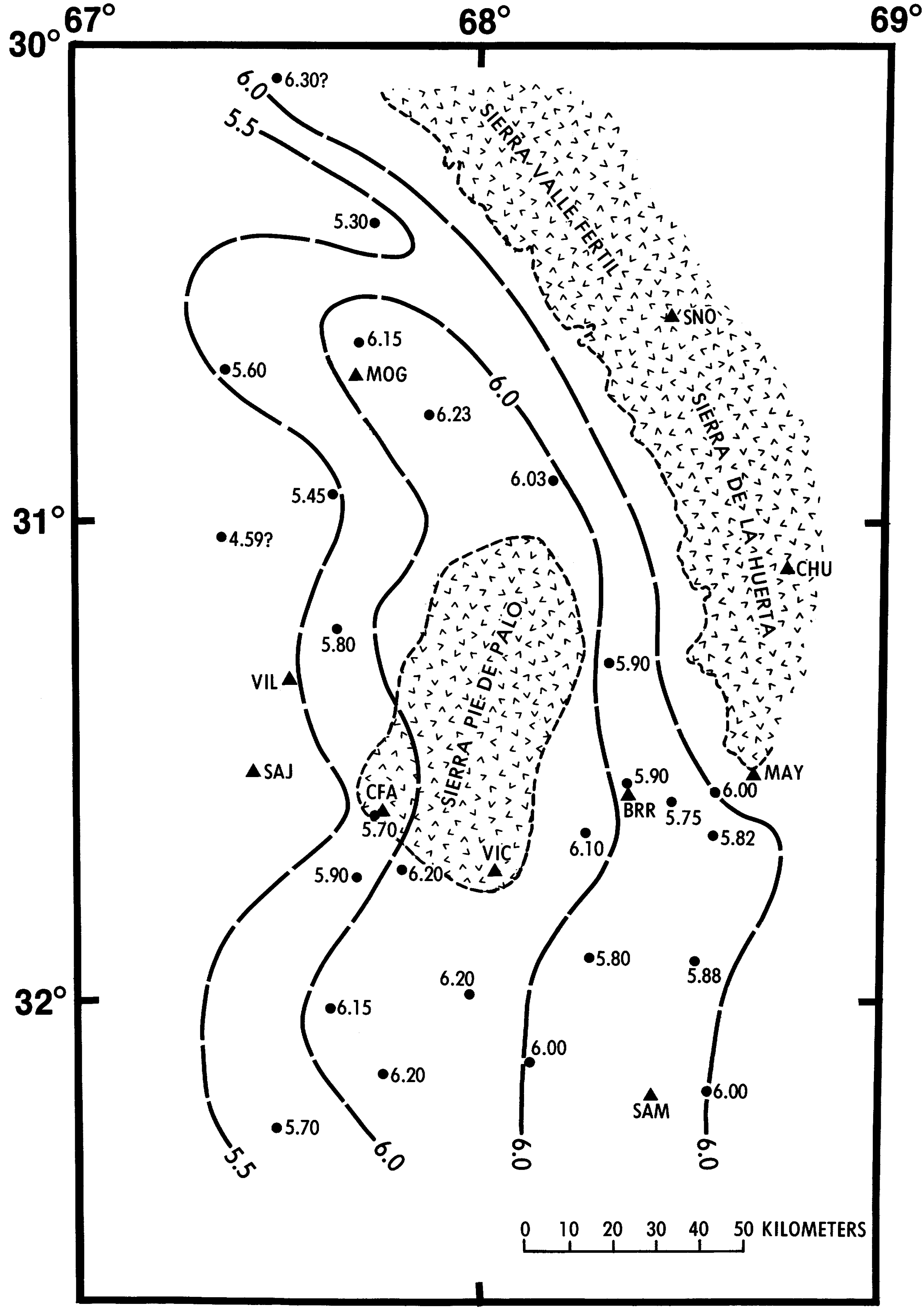

Figure 6. Uppermost Precambrian rock velocities, as determined by the refraction profile data (fig. 3), contoured in km/sec. Other symbols the same as in figure 3.

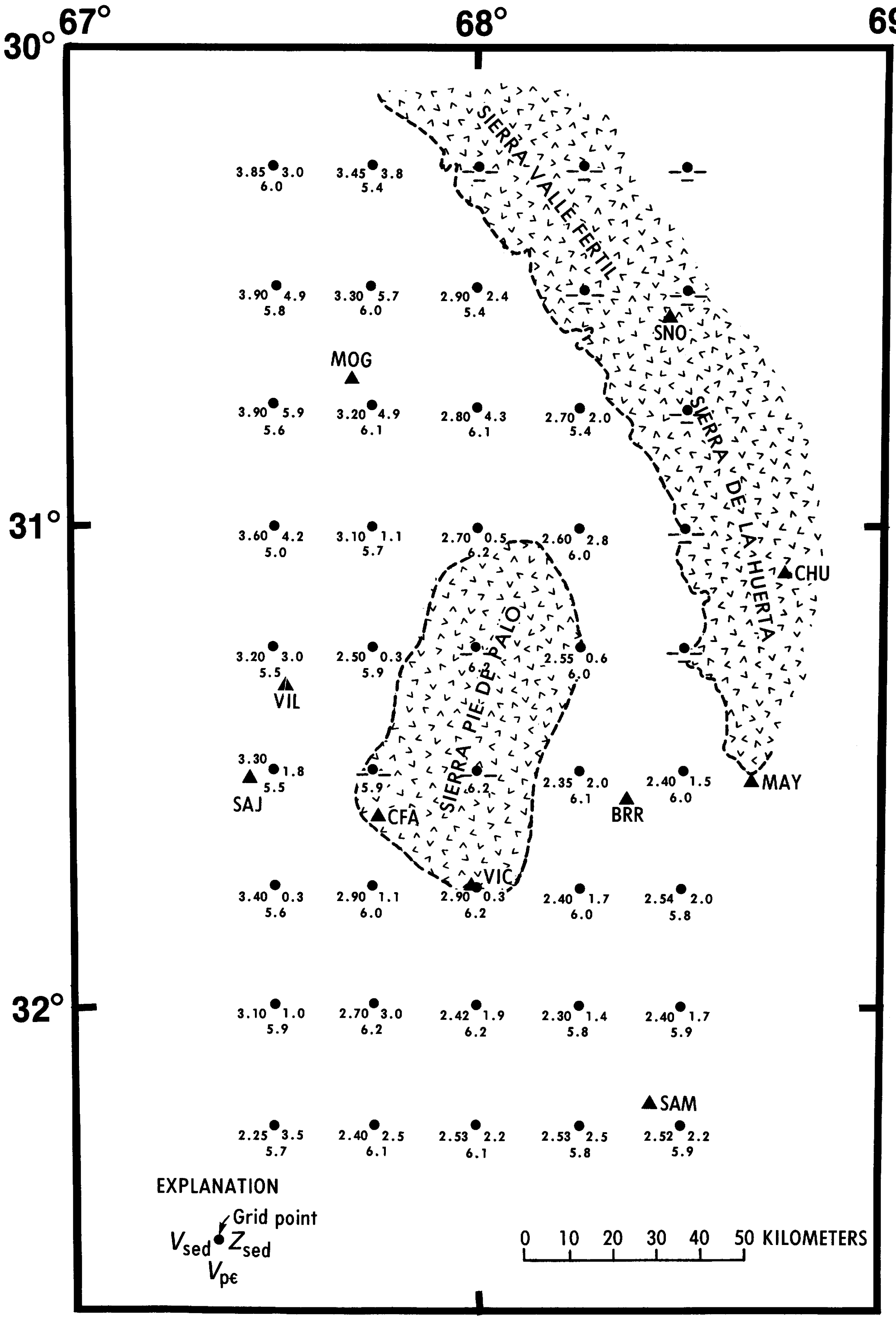

Figure 7. Grid map for velocities (sedimentary rocks $= V_{sed}$, Precambrian rocks $= V_{p\epsilon}$, both in km/sec) and sedimentary rock thicknesses (Z_{sed}, in km), as derived from figures 4, 5, and 6. Other symbols same as in figure 3.

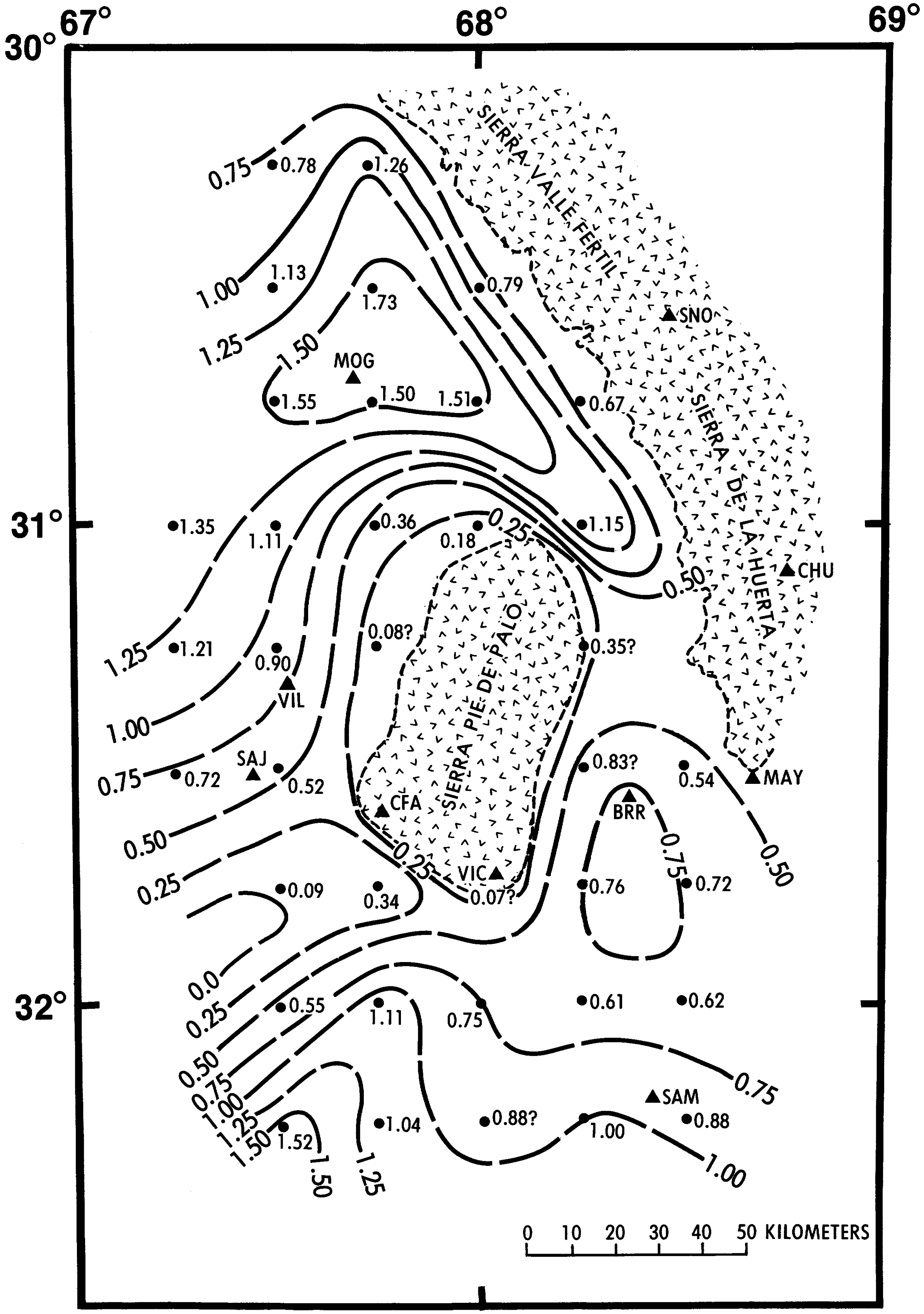

Figure 8. Sedimentary rock traveltimes (one-way vertical path), as calculated from the data shown in figures 4 and 5, contoured in seconds. Other symbols the same as figure 3.

Table 1. P-wave velocity model, Sierra Pie de Palo region of western Argentina

P-wave velocity (km/sec)	Thickness (km)	Depth to top of layer (km)
2.87	2.4	0
5.88	7.6	2.4
6.2	22.0	10.0
7.3	23.0	32.0
8.1	half-space	55.0

e. Precambrian travel time, $T_{pe}=Z_{pe}/V_{pe}=3.8$ km/6.0 km/sec=0.63 sec
f. "Actual" one-way travel time, $T_a=T_{sed}+T_{pe}=1.80$ sec+0.63 sec=2.43 sec
g. Station correction, $T_c=T_m$-T_a=2.13 sec-2.43 sec=-0.30 sec

T_c for MAY (Rock Site)

a. From figure 8, the sedimentary travel time, $T_{sed}=0.0$ sec (station located on Precambrian rock)
b. Sedimentary thickness, $Z_{sed}=0.0$
c. From figure 6, the Precambrian velocity, V_{pe}-6.0 km/sec
d. Thickness of Precambrian above 10 km, $T_{pe}=$ 10.0 km+station elevation=10.0 km+0.71 km=10.71 km
e. Precambrian travel time, T_{pe}-$Z_{pe}/V_{pe}=10.71$ km/6.0 km/sec=1.78 sec
f. "Actual" one-way travel time, $T_a=T_{sed}+T_{pe}=0.0$ sec+1.78 sec=1.78 sec
g. Station correction, $T_c=T_m$-T_a=2.13 sec-1.78 sec= +0.35 sec

A listing of the corrections derived in a similar manner for all network stations is given in table 2.

(3) *Station-delay Corrections, T_d*

The AVM station corrections almost certainly will not account for all of the travel time complexities within the region. Therefore, "station delay corrections," T_d, determined from the travel time residuals will also be applied in this study. Those corrections were calculated using the following procedure:

a. Select a 20-event subset from the entire sample of aftershocks of the November 23, 1977, Argentina earthquake that were recorded by the portable network. Those 20 events should be well recorded by all of the network stations and have epicenters that are well distributed throughout the aftershock zone and have depths greater than 10 km.
b. Locate the selected aftershocks using only the most precise arrival-time data available; that is, the P-wave arrival times from stations located on rock (CFA, VIC, MAY, CHU, and SNO) plus arrival-time data from VIL (for asimuthal control). Assume a P/S velocity ratio of 1.73 and use S-wave arrival times as recorded by the short-period horizontal seismographs at CFA. Apply the AVM station corrections. Results of this location process demonstrated that significant travel time residuals still remained at some stations located on alluvium, particularly MOG, BRR, and SAM. Thus, averages of the travel time residuals were determined for the individual network stations to serve as preliminary delay corrections, T_d.
c. Relocate the 20 selected events using their above preliminary-delay corrections and the S-wave arrival times recorded at rock site stations and using the Wood-Anderson instruments in San Juan (SAJ). Try various P/S velocity ratios to establish a value that tends to minimize the S-wave residuals and construct a Wadati plot using only the P and S-wave arrival

Table 2. Velocity model (AVM) station corrections, T_c, Argentina aftershock network

Station	Site Lithology	T_c correction (sec)
BRR	Sedimentary	+0.02
CFA	pЄ rock	+0.30
CHU	do.	+0.32
MAY	do.	+0.35
MOG	Sedimentary	-0.30
SAJ	do.	+0.03
SAM	do.	-0.09
SNO	pЄ rock	+0.30
VIC	do.	+0.40
VIL	Sedimentary	-0.03

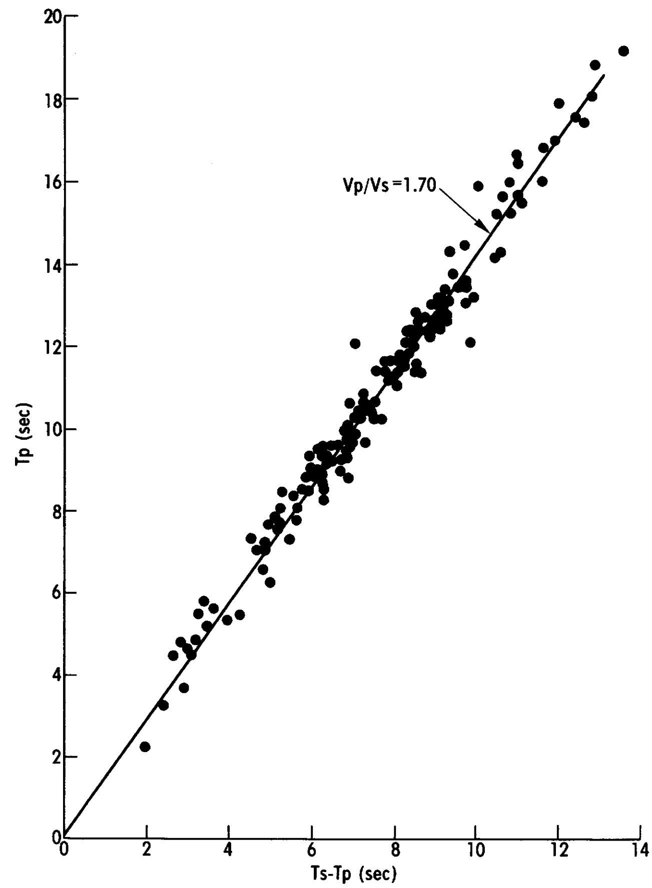

Figure 9. Wadati plot showing traveltimes of S-wave minus traveltimes of P-wave (Ts–Tp, sec) versus traveltime of P-wave (Tp, sec) for 20-event subset (refer to page 20). Data from the rock site stations.

Table 3. Station-delay corrections, T_d Argentina aftershock network

Station	Site Lithology	T_d Correction (sec)
BRR	Sedimentary	-0.27
CFA	p€ rock	+0.17
CHU	do.	0.00
MAY	do.	+0.14
MOG	Sedimentary	-0.97
SAJ	do.	0.00
SAM	do.	-0.39
SNO	p€ rock	0.00
VIC	do.	-0.01
VIL	Sedimentary	+0.38

Table 4. Final station corrections, T_s Argentina aftershock network

Station	Site Lithology	T_s, Correction (sec)
BRR	Sedimentary	-0.25
CFA	p€ rock	+0.47
CHU	do.	+0.32
MAY	do.	+0.49
MOG	Sedimentary	-1.27
SAJ	do.	+0.03
SAM	do.	-0.48
SNO	p€ rock	+0.30
VIC	do.	+0.39
VIL	Sedimentary	+0.35

times recorded at the rock sites (fig. 9). The result of both the P/S velocity ratio search and the Wadati plot was the selection of a value of 1.70.

d. To arrive at the final station delay corrections, T_d, relocate the 20-event subset of aftershocks using the 1.70 P/S velocity ratio and average the travel time residuals at each of the 10 stations. Table 3 presents the results of this procedure for the study area.

(4) *Final Station Corrections, T_s*
Obtain the algebraic sum of the AVM station corrections, T_c, and the "station delay" corrections, T_d, to estimate the "final" station corrections, T_s, as listed in table 4.

SUMMARY

The velocity model described in table 1 and the station corrections listed in table 4 were used in the HYPO71 program to locate the aftershocks of the western Argentina earthquake of November 23, 1977 (Langer and Bollinger, 1987). The average HYPO71 error measures for the aftershock hypocentral calculations were: RMS=0.12 sec; ERH=0.7 km; ERZ=1.3 km. We do not have a way to check for the presence of any systematic biases, but the use of high-quality S-wave data from CFA and SAJ eliminates the possibility of gross mislocations. Additionally, the depth distribution of the hypocenters (near surface to 30+ km; 110–135 km) given by Langer and Bollinger is the same as that derived from special seismicity studies of the region (Barazangi and Isacks, 1976). A full listing of the aftershock locational and error parameters is given in the appendix.

ACKNOWLEDGMENTS

Our appreciation is extended to the Instituto Nacional de Prevención Sismica (INPRES) and all personnel who contributed to our field monitoring program. Director Ing. Julio Aguirve Ruiz and staff seismologist, Dr. Juan C. Castano, provided assistance toward the necessary scientific and logistical support. We are also grateful to S. T. Algermissen for his coordination of this joint U.S.-Argentine postearthquake study. Ing. Abel E. Burna with YPF in Buenos Aires, Argentina, kindly provided the refraction profile data that were so important to our model development. Mr. David R. Toland of Cities Services Corporation, International Area, Houston, Tex., graciously provided the sonic logs for the two wells in the study area.

We also express gratitude to J. P. Whitcomb and R. F. Henrisey for their fieldwork and to Martha Adams, whose careful efforts obtained the basic data from the seismograms. M. J. Cecil and A. M. Rogers critically reviewed the manuscript and provided many helpful comments and suggestions.

REFERENCES CITED

Allmendinger, R. W., Jordan, T. E., Palma, M., and Isacks, B. L., 1983, Paleogeography and Andean structural geometry, northwest Argentina: Tectonics, 2, p. 1-16.

Baldis, B. A., and Febrer, J., 1983, Geodynamics of the Andean arc and related regions: *in* Geodynamics of the Eastern Pacific Region, Carribbean and Scotia Arcs, edited by Ramon Cabre, S. J., American Geophysical Union and Geological Society of America, Geodynamics Series, v. 9, p. 127-135.

Barazangi, M., and Isacks, B., 1976, Spatial distribution of earthquakes and subduction of the Nazca plate beneath South America: Geology, v. 4, p. 686-692.

Bastias, H. E., and Weidmann, N., 1983, Mapa de fallamiento moderno de la provincia de San Juan: Universidad Nacional de San Juan, Facultad de Ciencias Exactes, San Juan, Argentina, scale 1:500,000.

INPRES (Instituto Nacional de Prevención Sismica), 1977, El terremoto de San Juan del 23 de Noviembre de 1977, informe preliminar: Instituto Nacional de Prevención Sismica, San Juan, Republica Argentina, 101 p.

Jordan, T. E., Isacks, B. L., Allmendinger, R. W., Brewer, J. A., Ramos, V. A., and Ando, C. J., 1983, Andean tectonics related to geometry of subducted Nazca plate: Bulletin of the Geological Society of America, 94, p. 341-361.

Kadinsky-Cade, Katherine, Reilinger, Robert and Isacks, Bryan, 1985, Surface deformation associated with the November 23, 1977, Caucete Argentina earthquake sequence: Journal of Geophysical Research, v. 90, p. 12,691-12,700.

Langer, C. J., and Bollinger, G. A., 1988, Aftershocks of the western Argentina (Caucete) earthquake of 23 November 1977—some tectonic implications: Tectono-physics (in press).

Lee, W. H. K., Bennett, R. E. and Meagher, K. L., 1972, A method of estimating magnitude of local earthquakes from signal duration: U.S. Geological Survey Open-File Report 72-223, 28p.

Volponi, F. S., 1968, Los terremotos de Mendoza del 21 de Octubre de 1968 y la estructura de la corteza terrestre [The Mendoza earthquakes of 21 October 1968 and the structure of the earth's crust]: Acta Cuyana de Ingenieria, v. XII, Instituto Sismologico Zonda, Facultad de Ingenieria, Universidad Nacional de Cuyo, San Juan, Argentina, p. 95-110.

APPENDIX

List of aftershocks for the Argentina earthquake of November 23, 1977

Date (Dec. 1977)	Origin (UTC)	Lat. S (deg)	Long. W (deg)	Depth (km)	No. obs.[1]	DMIN[2] (km)	RMS[3]	Standard errors[4] DLAT (km)	DLON (km)	DZ (km)	QF[5]	M_D
06	1705 06.54	31.270	67.978	29.2	13	45	0.09	.24	0.22	0.66	B	4.7
06	1827 39.00	31.310	67.847	24.3	11	49	0.10	.43	.31	2.35	C	4.3
06	1932 27.99	31.285	67.953	28.5	12	45	0.13	.45	.38	.73	B	3.5
06	2336 32.45	31.265	67.969	27.3	10	46	0.08	.25	.33	.95	B	3.7
07	0200 32.82	31.140	67.737	7.5	11	47	0.08	.30	.51	2.01	C	3.6
07	0322 41.52	31.276	67.956	27.8	11	46	0.18	.56	.62	1.71	B	4.4
07	0409 55.42	31.576	67.529	13.1	12	19	0.15	.45	.57	1.80	B	3.3
07	0554 18.64	31.746	68.027	115.1	12	6	0.11	.78	.91	1.35	C	2.6
07	0655 46.13	31.694	67.939	30.0	11	5	0.10	.61	.37	.60	A	3.2
07	0802 19.84	31.837	67.836	17.7	10	16	0.08	.28	.35	.84	B	3.0
07	0807 09.89	31.038	67.803	2.4	13	53	0.12	.24	.29	.42	C	4.0
07	0817 29.49	31.827	67.737	17.1	10	24	0.07	.21	.25	1.01	B	4.1
07	0919 04.14	31.508	67.537	52.1	12	19	0.10	.35	.43	.95	A	2.5
07	0926 12.35	31.252	67.971	22.4	12	47	0.08	.24	.22	1.75	B	2.8
07	0941 45.25	31.297	67.966	26.8	14	43	0.12	.34	.29	.83	B	3.9
07	1130 27.97	31.837	67.743	8.9	11	24	0.09	.31	.28	.81	B	2.7
07	1413 06.22	31.456	67.468	19.9	11	15	0.17	.65	.95	2.50	B	2.4
07	1431 13.52	31.128	67.881	21.6	11	60	0.16	.50	.40	3.74	C	3.4
07	1509 39.03	31.276	67.833	21.3	11	53	0.08	.27	.28	2.17	C	3.2
07	1612 45.01	31.062	67.867	9.7	12	58	0.09	.25	.23	2.48	C	2.6
07	1705 40.21	31.580	67.734	31.1	11	28	0.15	.55	.52	.51	B	3.2
07	1720 12.82	31.822	67.808	15.0	13	18	0.14	.32	.34	1.37	B	3.1
07	1823 48.02	31.683	67.889	30.1	11	9	0.13	.66	.66	.74	A	2.8
07	1835 12.65	31.114	67.798	7.8	14	52	0.08	.16	.19	.75	C	2.7
07	2012 27.47	31.640	67.913	28.5	11	12	0.08	.36	.24	.49	A	2.9
07	2016 14.10	31.780	67.803	22.4	12	16	0.09	.25	.25	.57	B	3.1
07	2029 13.52	31.509	67.869	22.4	11	27	0.11	.46	.32	1.47	B	3.2
07	2033 27.85	31.269	67.845	9.5	10	53	0.13	.46	.46	4.02	C	2.8
07	2137 16.22	31.043	67.782	4.4	12	51	0.10	.23	.22	3.63	C	3.2
07	2252 29.34	31.792	67.833	21.3	11	14	0.15	.47	.47	.81	B	3.0
08	0224 36.05	31.136	67.907	23.8	12	58	0.11	.29	.30	1.27	C	2.7
08	0416 05.64	31.527	67.577	13.9	12	23	0.07	.23	.24	1.30	B	3.0
08	0625 05.09	31.231	67.803	7.9	11	55	0.12	.38	.62	2.34	C	3.3
08	1103 28.38	31.800	67.854	24.0	11	13	0.10	.35	.42	.61	B	3.2
08	1202 26.51	31.421	67.874	7.4	10	36	0.08	.44	.31	1.79	B	3.2
08	1251 44.76	31.679	67.891	28.3	11	10	0.16	.60	.60	.89	B	2.6
08	1338 23.41	31.274	67.915	24.5	11	48	0.13	.47	.34	2.42	B	3.3
08	1505 31.44	31.077	67.853	23.8	11	58	0.11	.33	.33	1.45	C	3.2
08	1734 21.13	31.260	67.832	2.3	10	55	0.13	.46	.31	.61	C	3.0
08	1831 47.60	31.560	67.079	134.0	13	25	0.16	.85	1.32	1.26	C	2.7
08	1834 51.93	31.285	67.966	25.8	12	44	0.08	.20	.19	.80	B	3.0
08	1904 43.57	31.458	68.022	28.2	10	26	0.08	.31	.21	.48	A	3.2
08	1952 15.33	31.234	67.752	8.0	12	50	0.10	.22	.42	1.37	B	3.8
08	2046 35.61	31.007	67.797	5.2	12	53	0.05	.12	.12	.67	C	2.5
08	2321 28.35	31.051	67.795	19.5	13	52	0.09	.20	.30	2.89	C	2.1
09	0038 07.40	31.451	67.979	31.9	12	30	.13	.49	.37	.48	A	3.3
09	0102 28.70	31.382	67.803	8.0	11	42	0.13	.55	.33	1.52	B	3.3
09	0131 59.19	31.197	67.845	1.6	12	58	0.18	.46	.43	.71	C	2.9
09	0248 58.05	31.509	67.705	30.4	11	35	0.09	.32	.35	.38	B	3.3
09	0511 31.44	31.146	67.722	2.6	12	45	0.06	.16	.14	2.08	C	2.7
09	0716 54.56	31.058	68.003	1.7	13	49	0.14	.26	.29	.42	B	2.8
09	0825 21.78	31.034	67.800	8.0	10	53	0.08	.23	.26	1.02	C	2.7
09	0918 12.34	31.502	67.690	31.3	11	34	0.12	.50	.39	.45	B	3.0
09	1036 03.65	31.777	67.969	10.8	12	4	0.06	.20	.15	.37	B	3.3
09	1220 11.19	31.121	67.746	7.0	13	47	0.11	.30	.42	1.51	B	2.7
09	1244 47.41	31.247	67.988	28.0	12	46	0.18	.49	.52	1.68	B	3.2
09	1519 45.19	31.272	67.980	25.6	14	45	0.08	.20	.21	.76	B	3.7
09	1842 54.79	31.098	67.864	6.5	11	57	0.14	.46	.37	1.87	C	2.3
09	1856 09.65	31.491	67.727	31.6	11	13	0.15	.79	.58	.72	A	2.7
09	2032 27.03	30.988	67.875	9.2	13	52	0.15	.35	.38	2.94	C	3.1
09	2057 52.90	31.303	67.968	27.6	13	42	0.12	.33	.32	1.01	B	2.9
09	2144 48.19	31.615	67.839	12.8	15	18	0.11	.27	.24	.87	B	4.2
09	2247 39.93	31.348	67.868	4.8	12	33	0.12	.42	.29	1.93	B	3.8
09	2310 48.66	31.564	67.968	30.5	12	19	0.13	.75	.52	.72	A	3.3

List of aftershocks for the Argentina earthquake of November 23, 1977—*Continued*

Date (Dec. 1977)	Origin (UTC)		Lat. S (deg)	Long. W (deg)	Depth (km)	No. obs.[1]	DMIN[2] (km)	RMS[3]	Standard errors[4] DLAT (km)	DLON (km)	DZ (km)	QF[5]	M_D
10	0030	33.21	31.416	67.908	16.8	12	31	0.13	.49	.33	2.87	B	3.1
10	0055	22.91	31.142	67.819	6.3	14	51	0.09	.21	.18	.91	C	3.0
10	0140	25.74	31.057	68.012	6.2	14	49	0.06	.13	.19	.59	B	3.5
10	0256	41.61	31.833	67.828	24.7	12	17	0.09	.29	.33	.63	B	3.2
10	0413	19.42	31.526	67.758	28.5	12	13	0.09	.38	.25	.58	A	2.9
10	0433	57.69	30.913	69.006	110.9	16	69	0.27	1.50	2.16	1.98	D	3.6
10	0436	18.77	31.112	67.859	6.8	15	55	0.07	.14	.13	.47	C	3.1
10	0519	38.23	31.463	67.636	41.0	12	12	0.08	.48	.28	1.02	A	3.3
10	0704	17.20	31.743	67.936	10.1	13	3	0.10	.32	.30	.30	B	3.7
10	0711	51.12	31.225	67.690	25.9	15	39	0.12	.28	.32	1.27	B	4.1
10	0719	20.84	31.135	67.771	23.1	12	50	0.10	.26	.29	1.26	B	3.3
10	0836	56.29	31.261	67.708	25.4	12	35	0.08	.25	.28	1.42	B	4.2
10	1010	29.48	31.097	67.938	22.8	14	56	0.08	.18	.18	1.07	C	3.5
10	1016	12.99	31.579	67.849	14.2	12	21	0.18	.78	.48	2.44	B	3.8
10	1131	07.32	31.495	67.745	30.2	12	14	0.17	.67	.47	.74	B	2.8
10	1250	13.21	31.741	67.968	27.2	10	0	0.17	.74	.70	.84	C	2.8
10	1314	05.48	31.397	68.668	112.1	17	18	0.16	.77	1.07	1.01	C	3.2
10	1419	54.63	31.249	67.735	27.7	13	37	0.12	.39	.42	1.89	B	4.0
10	1446	29.23	31.250	67.726	20.9	13	37	0.06	.17	.21	1.39	B	3.3
10	1448	06.24	31.250	67.715	21.5	13	36	0.14	.43	.46	2.94	B	3.1
10	1504	33.02	31.615	67.959	30.2	11	14	0.20	1.42	.96	1.24	B	2.3
10	1839	07.73	31.126	67.917	23.2	14	56	0.13	.32	.32	1.67	C	3.7
10	1926	04.85	31.856	67.705	16.4	10	28	0.24	.74	1.09	3.99	B	3.0
10	1929	51.89	31.370	67.948	23.8	12	37	0.19	.84	.55	3.36	B	2.7
10	2047	34.09	31.778	67.490	23.1	13	27	0.11	.31	.35	1.07	B	3.3
10	2100	19.72	31.058	67.951	6.4	11	52	0.09	.25	.22	.96	C	3.5
10	2158	07.95	31.758	67.680	26.8	12	21	0.10	.30	.29	.61	B	3.4
10	2315	10.57	31.229	67.740	19.9	13	39	0.09	.23	.28	2.16	B	3.6
11	0044	25.34	31.163	67.814	8.4	13	48	0.12	.29	.27	1.51	B	3.8
11	0327	12.73	31.038	67.802	6.2	13	53	0.09	.30	.25	1.36	C	3.3
11	0447	31.72	31.645	68.200	48.1	13	6	0.16	.71	.84	1.80	C	2.2
11	0452	55.89	31.528	67.785	31.6	13	15	0.09	.46	.27	.37	A	2.7
11	0531	53.92	31.076	67.940	5.8	14	55	0.09	.23	.22	.98	C	3.3
11	0705	02.42	31.703	67.791	10.0	12	17	0.14	.40	.35	.77	B	3.4
11	0707	08.36	31.151	67.728	16.7	13	46	0.06	.13	.23	2.24	C	3.1
11	0758	17.41	31.271	68.757	116.1	16	28	0.19	1.06	1.25	1.44	C	2.4
11	0945	09.35	31.168	67.788	6.8	14	47	0.14	.29	.39	1.46	B	3.4
11	0950	36.56	31.833	67.788	11.7	9	20	0.13	.49	.60	3.01	C	2.6
11	0958	59.98	31.767	67.770	20.9	13	19	0.09	.27	.26	.65	B	3.2
11	1038	10.17	31.267	67.951	6.9	13	45	0.08	.24	.18	.73	B	3.0
11	1044	40.43	31.173	67.776	16.5	14	46	0.07	.15	.20	2.50	C	3.4
11	1046	53.67	31.080	67.891	22.9	13	58	0.10	.28	.23	1.38	C	3.0
11	1102	12.24	31.140	67.985	25.9	11	51	0.13	.39	.40	1.55	B	3.3
11	1246	21.60	31.425	67.733	27.4	13	19	0.10	.50	.27	.73	B	2.4
11	1331	04.23	31.479	67.655	34.2	12	10	0.11	.52	.43	1.04	A	2.9
11	1402	23.51	31.277	67.893	2.0	11	41	0.10	.28	.25	.42	B	3.0
11	1430	43.87	31.366	67.728	14.1	15	24	0.15	.42	.33	3.66	B	3.0
11	1617	11.37	31.413	67.704	9.8	14	19	0.13	.37	.31	.96	B	2.9
11	1626	00.07	31.415	67.699	11.5	13	18	0.10	.30	.26	1.97	B	3.3
11	1640	44.21	31.505	67.781	28.6	12	16	0.13	.56	.36	.87	A	3.3
11	1643	19.07	31.418	67.709	9.7	13	18	0.11	.32	.28	.79	B	3.0
11	1745	50.14	31.828	67.761	21.3	13	22	0.09	.25	.29	.60	B	2.9
11	1857	57.32	31.520	67.867	13.2	13	23	0.19	.80	.44	3.82	B	3.6
11	1934	24.03	31.116	67.856	23.0	13	55	0.07	.18	.17	.87	C	2.9
11	2121	55.83	31.538	67.730	31.1	12	10	0.13	.60	.46	.52	A	2.7
11	2128	13.25	31.084	67.816	8.7	13	54	0.09	.20	.24	1.80	C	2.6
11	2231	59.78	31.553	67.634	31.3	12	2	0.13	.52	.46	.47	A	3.1
11	2300	56.10	31.075	67.995	22.1	14	51	0.09	.21	.21	1.21	C	2.8
11	2333	08.34	31.359	67.697	28.6	11	24	0.20	1.00	.68	1.60	B	2.9
12	0043	29.00	31.032	67.802	1.7	12	53	0.09	.23	.23	.50	C	3.8
12	0114	45.01	31.801	67.833	22.0	13	14	0.07	.20	.22	.37	B	3.6
12	0215	38.32	31.277	67.918	27.5	12	42	0.07	.21	.19	.65	B	3.5
12	0304	45.28	31.517	68.868	110.0	16	30	0.16	.93	1.46	.95	C	2.7
12	0412	45.04	31.266	67.986	26.3	12	45	0.10	.28	.28	.94	B	2.7
12	0443	24.41	31.503	67.730	30.6	12	12	0.05	.19	.18	.19	A	2.5
12	0556	13.62	31.353	67.835	20.6	13	31	0.12	.41	.32	2.58	B	3.1
12	0611	22.57	31.466	67.666	8.8	12	12	0.16	.63	.48	1.32	B	3.3
12	0819	52.39	31.817	67.828	17.2	11	16	0.16	.48	.60	1.54	C	2.4
12	0916	14.94	31.574	67.502	16.5	12	12	0.09	.28	.34	.86	B	2.9
12	1029	00.95	31.194	67.724	6.0	13	43	0.14	.48	.48	2.14	C	2.8

List of aftershocks for the Argentina earthquake of November 23, 1977—*Continued*

Date (Dec. 1977)	Origin (UTC)	Lat. S (deg)	Long. W (deg)	Depth (km)	No. obs.[1]	DMIN[2] (km)	RMS[3]	Standard errors[4] DLAT (km)	DLON (km)	DZ (km)	QF[5]	M_D
12	1244 24.77	31.120	67.779	1.6	14	50	0.11	.22	.28	.39	C	3.1
12	1342 42.09	31.208	67.694	20.0	11	40	0.09	.34	.30	2.14	C	3.1
12	1346 00.55	31.119	67.766	2.5	12	49	0.08	.19	.19	2.89	C	2.9
12	1510 01.99	31.201	67.708	16.7	13	41	0.13	.35	.42	3.80	C	3.2
12	1517 48.25	31.392	67.864	20.9	12	30	0.18	.71	.47	3.51	B	3.0
12	1602 29.29	31.208	67.708	20.8	14	41	0.14	.39	.50	2.85	B	3.9
12	1715 16.52	31.482	67.482	14.7	11	15	0.09	.31	.33	1.04	A	2.5
12	1748 28.64	31.198	67.698	15.7	12	42	0.08	.28	.32	2.78	C	2.9
12	1908 36.22	31.209	67.701	24.3	12	41	0.16	.50	.56	3.15	B	2.4
12	2044 16.60	31.246	67.767	23.4	12	38	0.13	.45	.38	3.79	B	2.7
12	2056 32.39	31.577	67.720	30.8	13	9	0.09	.24	.28	.25	A	3.2
12	2307 10.58	31.566	67.922	7.0	12	19	0.17	.58	.51	1.93	C	3.2
12	2318 23.11	31.846	67.892	19.3	13	14	0.09	.29	.28	.73	B	3.7
12	2331 51.74	31.470	67.736	30.7	12	15	0.08	.38	.32	.40	A	3.0
13	0033 09.95	31.574	67.673	5.3	14	4	0.13	.50	.36	1.10	B	3.1
13	0220 57.35	31.268	67.708	26.9	14	34	0.14	.32	.35	1.07	B	2.8
13	0304 36.21	31.385	67.702	30.3	13	21	0.09	.33	.27	.42	A	2.8
13	0341 55.31	31.222	67.753	5.7	14	40	0.10	.32	.26	1.30	B	2.9
13	0744 12.44	31.866	67.849	18.0	12	18	0.09	.28	.31	.87	B	3.5
13	0802 11.80	31.559	67.641	34.6	12	1	0.12	.47	.44	.86	A	3.1
13	0845 40.12	31.519	67.608	34.6	13	6	0.15	.60	.53	.99	A	2.3
13	1006 17.79	31.699	67.523	23.2	14	18	0.13	.35	.39	.65	B	4.3
13	1100 26.53	31.785	67.811	9.3	11	16	0.12	.33	.46	.98	B	2.7
13	1424 04.99	31.124	67.830	7.0	13	53	0.12	.28	.34	1.54	C	3.8
13	1552 50.28	31.355	67.862	23.0	12	32	0.15	.55	.39	2.75	B	3.7
13	1620 26.83	31.231	67.772	15.2	13	40	0.10	.29	.28	3.90	C	3.6
13	1722 54.94	31.709	67.507	16.9	13	20	0.07	.20	.19	.74	B	2.7
13	1845 45.76	31.757	67.774	21.6	11	18	0.13	.41	.36	.77	B	2.7
13	1851 45.73	31.570	67.861	12.0	12	21	0.13	.50	.29	2.18	B	3.4
13	1904 15.08	31.666	67.738	23.8	12	15	0.15	.52	.42	.85	B	2.5
13	1919 21.58	31.773	67.795	24.5	13	17	0.09	.26	.26	.52	B	2.8
13	2325 54.29	31.652	67.591	11.0	12	10	0.06	.18	.16	.81	B	3.5
14	0230 35.57	31.811	67.835	22.8	12	15	0.13	.42	.41	.79	B	2.9
14	0344 53.99	31.673	68.044	30.7	12	10	0.15	.85	.65	.59	C	2.4
14	0352 42.24	31.645	67.750	13.7	11	14	0.10	.30	.26	1.04	B	2.2
14	1124 30.31	31.139	67.911	22.6	15	55	0.09	.19	.21	1.12	C	3.2
14	1404 11.65	31.713	67.869	29.9	12	10	0.17	.66	.57	.74	B	2.4
14	1742 55.11	31.111	67.767	8.1	12	49	0.07	.18	.22	.86	B	3.1
14	2217 08.00	31.637	69.029	116.1	16	46	0.16	1.32	1.32	1.13	C	2.9
15	0417 25.16	31.585	67.727	29.2	14	9	0.13	.39	.36	.55	A	3.0
15	0436 33.23	31.132	67.911	8.4	13	55	0.07	.17	.17	1.41	C	3.0
15	0724 57.89	31.316	67.902	27.0	15	38	0.11	.28	.26	.88	B	3.8
15	0751 21.62	31.838	67.831	13.2	15	17	0.11	.26	.28	1.15	B	3.5
15	0803 38.56	31.493	68.722	122.2	18	16	0.16	.86	1.15	.97	C	2.8
15	0958 24.94	31.122	67.837	6.6	14	53	0.08	.16	.16	.59	C	3.7
15	1034 02.60	31.099	67.894	22.5	14	58	0.08	.17	.19	.93	C	2.9
15	1425 40.98	31.581	67.717	29.5	12	29	0.07	.22	.23	.36	A	3.2
15	1640 23.56	31.611	67.704	29.2	12	28	0.10	.32	.33	.54	B	3.3
15	1744 59.03	31.216	67.828	5.8	12	56	0.11	.42	.29	1.74	C	3.2
15	1913 49.18	31.228	68.444	116.0	13	12	0.09	.60	.64	.91	B	2.6
15	2234 28.64	31.242	67.841	9.3	12	41	0.06	.19	.15	1.32	B	3.2
15	2258 04.85	31.831	67.847	18.1	13	15	0.13	.36	.38	.96	B	2.7
15	2320 37.86	31.194	67.719	24.2	13	42	0.12	.29	.36	1.18	B	3.2
16	0447 02.10	31.747	68.007	28.1	13	4	0.12	.45	.42	.46	B	3.2
16	0553 01.24	31.419	67.669	33.6	12	17	0.13	.63	.48	1.59	A	3.2
16	1018 35.84	31.549	67.513	9.8	9	11	0.25	1.37	1.41	2.50	C	2.9
16	1106 45.45	31.170	67.905	25.9	12	51	0.09	.28	.24	1.08	B	3.3
16	1215 33.30	31.461	67.617	39.1	13	12	0.05	.25	.18	.59	A	3.1
16	1249 44.28	31.798	67.939	16.5	10	7	0.21	.91	.88	3.26	C	2.9
17	0202 37.85	31.235	67.919	26.3	13	46	0.09	.25	.22	.94	B	3.7

[1] No. obs.--the number of observations used to obtain hypocentral solutions.

[2] DMIN--distance to the closest seismograph station.

[3] RMS--root mean square errors of travel-time residuals.

[4] Standard errors--the indices of precision relating to the values and distribution of the unknown errors in the hypocentral solution where DLAT=error in latitude, DLON=error in longitude, and DZ=error in depth.

[5] QF--a measure that is intended to indicate the general reliability of the hypocentral solution where A = excellent epicenter, good focal depth; B=good epicenter, fair focal depth; C=fair epicenter, poor focal depth; D=poor epicenter, poor focal depth.

[6] M_D--Local magnitude estimate of aftershock (Lee and others, 1972).

★ U.S. GPO: 573-047/66,066 /1988